Supporting Information

Reforming of methane with carbon dioxide over cerium oxide promoted nickel nanoparticles deposited on 4-channel hollow fibers by atomic layer deposition

Baitang Jin,[a] Zeyu Shang,[a] Shiguang Li,[b] Ying-Bing Jiang,[c] Xuehong Gu,[d] and Xinhua Liang*[a]

[a] *Department of Chemical and Biochemical Engineering, Missouri University of Science and Technology, Rolla, Missouri 65409, United States*

[b] *Gas Technology Institute, 1700 South Mount Prospect Road, Des Plaines, IL 60018, United States*

[c] *TEM Laboratory, University of New Mexico, Albuquerque, New Mexico 87131, United States*

[d] *State Key Laboratory of Materials-Oriented Chemical Engineering, College of Chemistry and Chemical Engineering, Nanjing Tech University, 5 Xinmofan Road, Nanjing 210009, P.R. China*

* Corresponding author. Email: liangxin@mst.edu

Experimental

$NiAl_2O_4$ was synthesized by the co-precipitation method following the method in Referenc.[1] An aqueous solution of $Ni(NO_3)_2 \cdot 6H_2O$ and $Al(NO_3)_3 \cdot 9H_2O$ was mixed with ammonium hydroxide drop by drop. After filtration, the sample was washed with deionized water, dried in an oven at 100 °C for 12 h, and calcined in air at 900 °C for 5 h to obtain $NiAl_2O_4$.

CeO_2-$NiAl_2O_4$ (with 5 wt.% Ce) was synthesized by the incipient wetness (IW) method. The synthesized $NiAl_2O_4$ was added to an aqueous solution of $Ce(NO_3)_3 \cdot 6H_2O$ and dried at 100 °C, followed by calcination in air at 500 °C for 5 h.

Ce/Al_2O_3 (with 1.5 wt.% Ce) was synthesized by the incipient wetness method. Al_2O_3 was added to an aqueous solution of $Ce(NO_3)_3 \cdot 6H_2O$ and dried at 100 °C, followed by calcination in air at 500 °C for 5 h.

NiO was synthesized by calcining $Ni(NO_3)_2 \cdot 6H_2O$ in air at 500 °C for 3 h.

To compare the effects of reduction temperature, Ni/Al_2O_3NP-ALD was calcined in air at 500 °C for 3 h (using the same calcination procedure as the IW method for $CeNi/Al_2O_3$NP-ALD). This sample was named as cal-Ni/Al_2O_3NP-ALD.

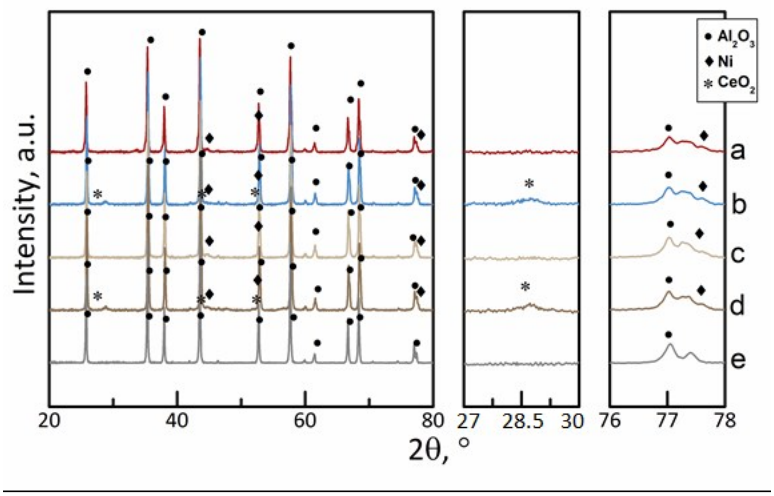

Figure S1. XRD patterns of reduced (a) Ni/Al_2O_3NP-ALD, (b) $CeNi/Al_2O_3$NP-ALD, (c) Ni/Al_2O_3NP-IW, (d) $CeNi/Al_2O_3$NP-IW, and (e) Al_2O_3NP.

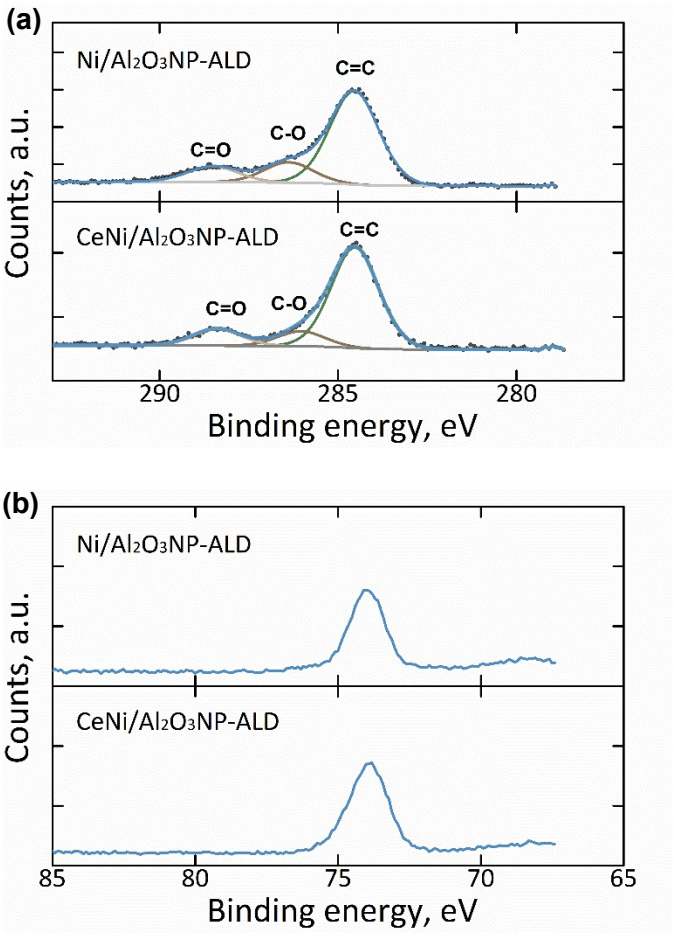

Figure S2. XPS core levels of (a) C 1s and (b) Al 2p of Ni/Al_2O_3NP-ALD and CeNi/Al_2O_3NP-ALD.

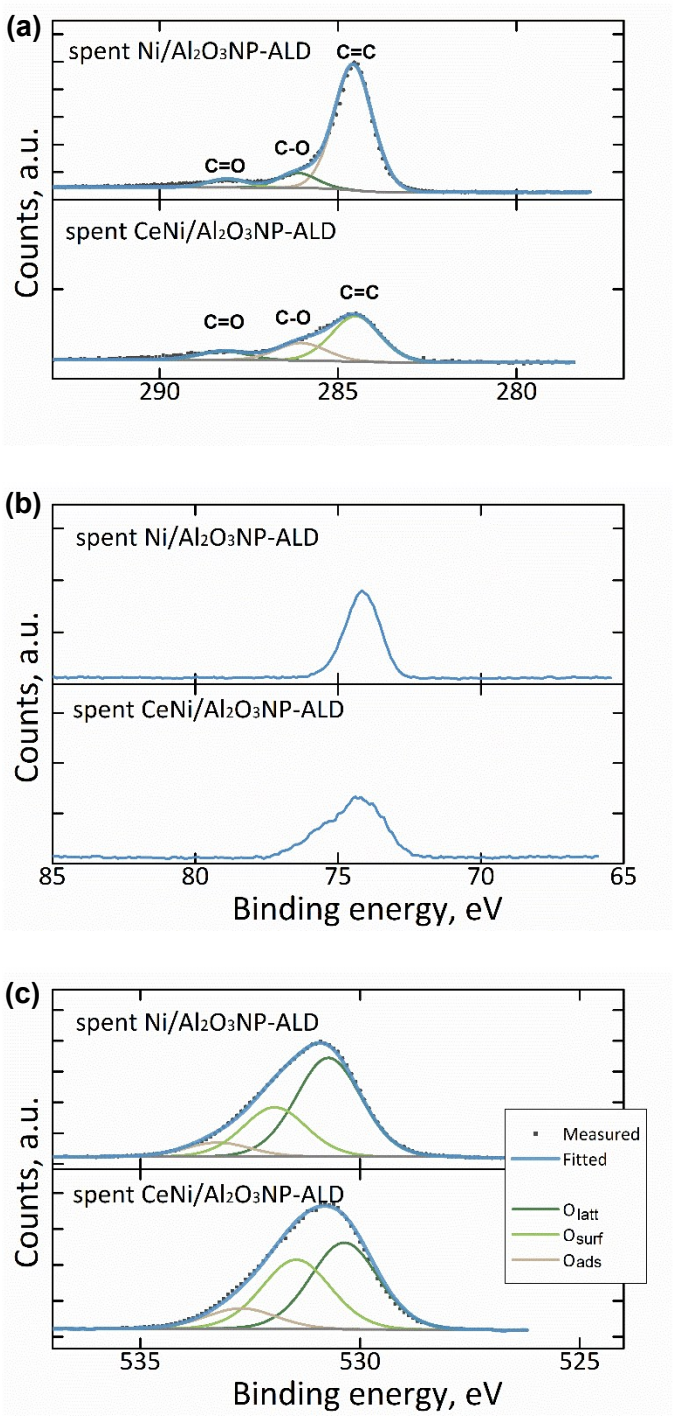

Figure S3. XPS core levels of (a) C 1s, (b) Al 2p, and (c) O 1s of spent Ni/Al_2O_3NP-ALD and spent $CeNi/Al_2O_3$NP-ALD samples after DRM at 850 °C for 72 h.

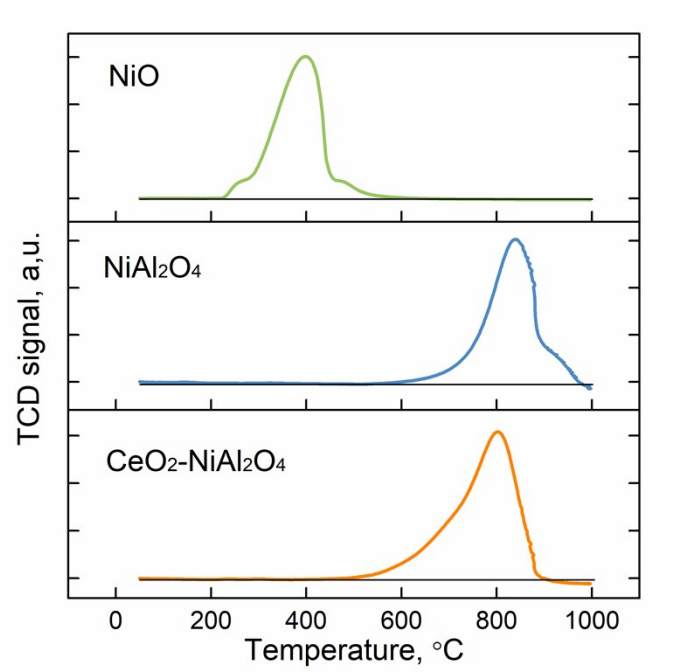

Figure S4. H_2-TPR profiles of NiO, $NiAl_2O_4$, and CeO_2-$NiAl_2O_4$.

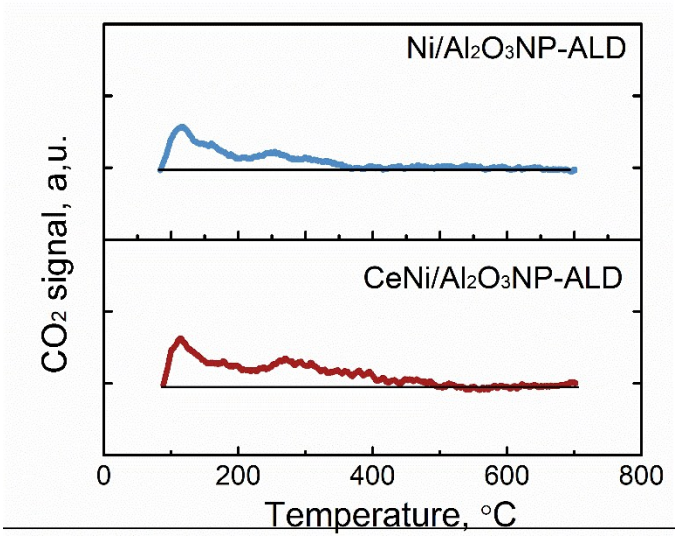

Figure S5. CO_2-TPD of Ni/Al_2O_3NP-ALD and $CeNi/Al_2O_3$NP-ALD.

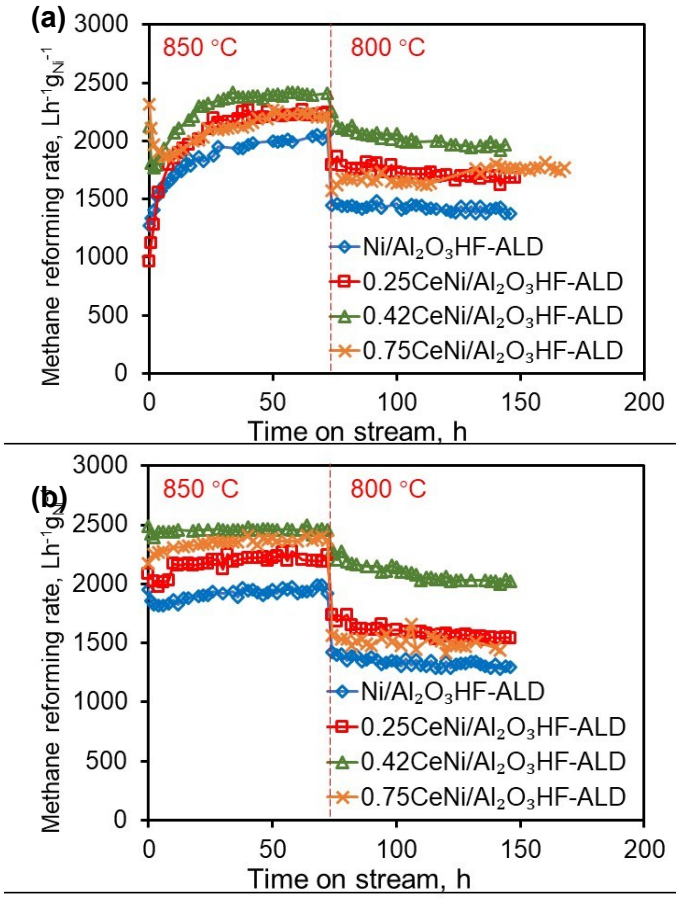

Figure S6. Methane reforming rate of (a) the first cycle and (b) the second cycle of dry reforming of methane reactions catalyzed by $Ni/Al_2O_3HF\text{-}ALD$, $0.25CeNi/Al_2O_3HF\text{-}ALD$, $0.42CeNi/Al_2O_3HF\text{-}ALD$, and $0.75CeNi/Al_2O_3HF\text{-}ALD$. Reaction conditions: catalyst loading of 0.6 g, 0.11 wt.% Ni, reactant composition of CH_4/CO_2=50/50 vol. %, and total flow rate of 60 mL/min.

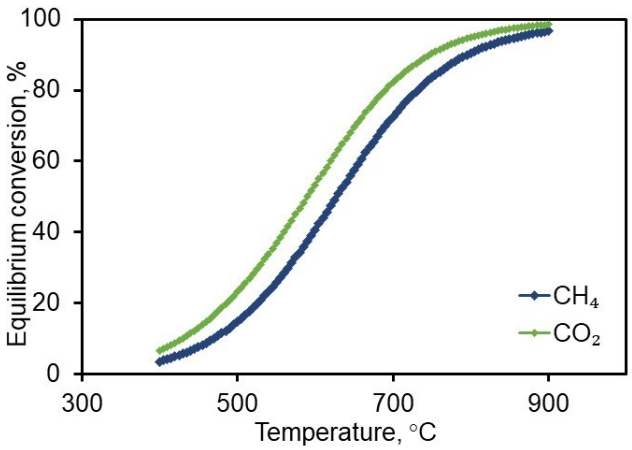

Figure S7. Thermodynamic equilibrium conversion of CO_2 and CH_4 as a function of temperature with an inlet mole ratio of CH_4/CO_2=1 at atmosphere pressure.

Thermodynamic equilibrium conversions of CH_4 and CO_2 were calculated with the RGibbs reactor module, using AspenONE 10 with SRK as the equation of state. CH_4, CO_2, CO, H_2, and H_2O were involved in the system. Assumptions were made that there was no carbon formation in the reaction system and there was no pressure drop for the RGibbs reactor. Inlet gas was set as CH_4/CO_2=1 (mole ratio) and the pressure was set at atmosphere pressure. Because there was only negligible amount of carbon deposition in our experiment, the carbon deposition was not considered in this calculation. In addition, other theoretical by-product species, such as CH_3OH or C_2H_6, were not detected in our GC, so these species were not considered in the equilibrium calculation either. By minimizing the Gibbs free energy of the system, the equilibrium conversions of CH_4 and CO_2 were calculated.

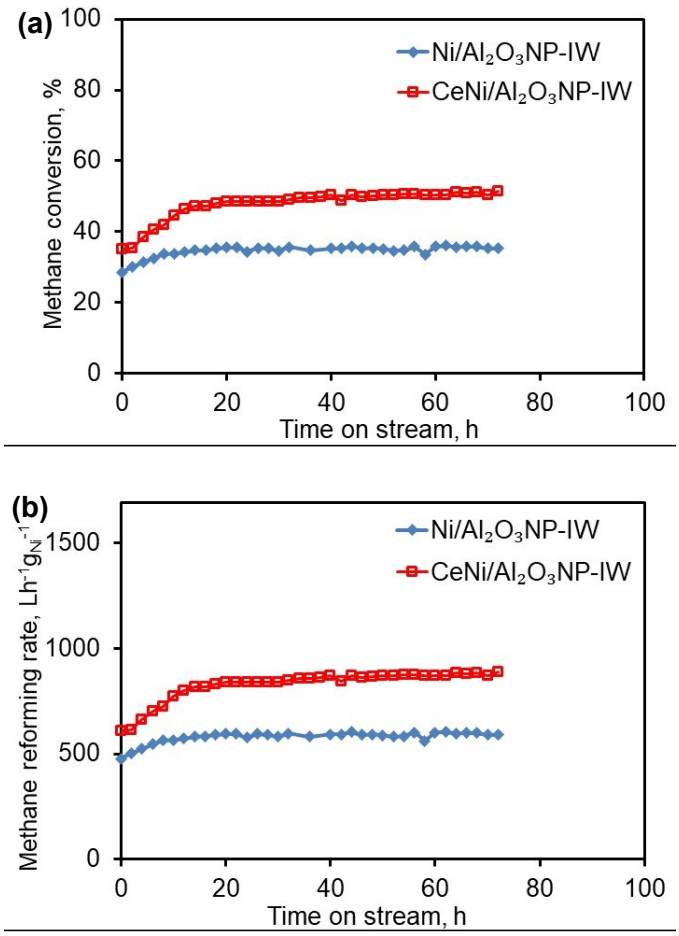

Figure S8. (a) Methane conversion and (b) methane reforming rate of the dry reforming of methane reactions catalyzed by $CeNi/Al_2O_3NP$-IW and Ni/Al_2O_3NP-IW at 850 °C. Reaction conditions: catalyst loading of 0.070 g, 1.50 wt.% Ni, reactant composition of CH_4/CO_2=50/50 vol. %, and total flow rate of 60 mL/min.

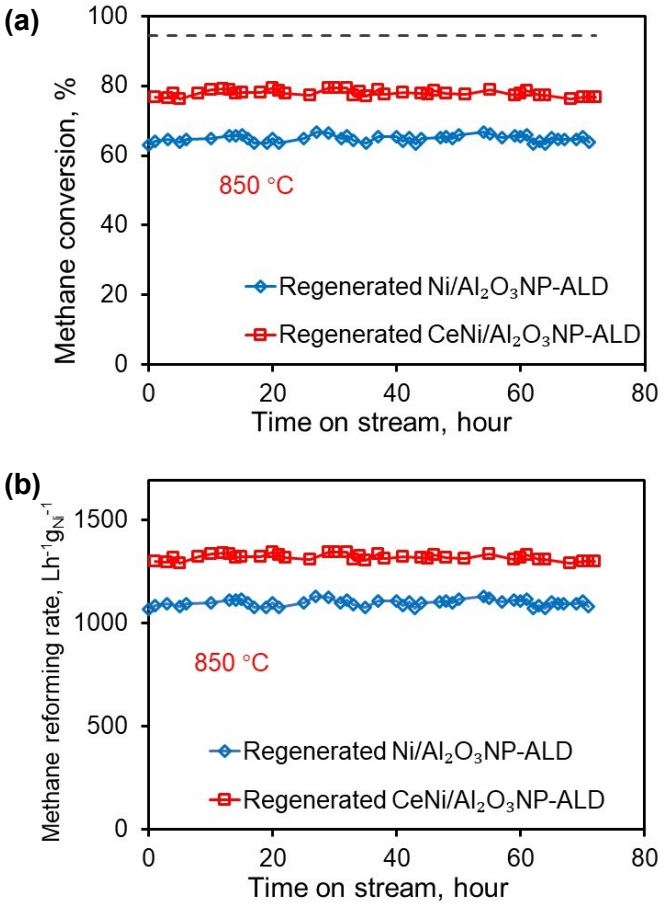

Figure S9. (a) Methane conversion and (b) methane reforming rate of the second cycle of dry reforming of methane reactions catalyzed by regenerated $CeNi/Al_2O_3NP$-IW and regenerated Ni/Al_2O_3NP-IW at 850 °C. Reaction conditions: catalyst loading of 0.070 g, 1.49 wt.% Ni, reactant composition of CH_4/CO_2=50/50 vol. %, and total flow rate of 60 mL/min.

Thermodynamic analysis of phase transform during reaction

To figure out the reaction of solid phase change, Gibbs free energy was calculated using (equ.1) with the standard Gibbs free energy of formation based on Reference,[2] as shown in Figure S10.

The perovskite $CeAlO_3$ was reported to be highly stable under a reducing atmosphere at high temperature. It was possible that Ce^{3+} ion doped into the Al_2O_3 (R1) or $NiAl_2O_4$ (R2) lattice and, thereby, formed a thermally stable $CeAlO_3$. During the latter process, Ni^{2+} ions might have been driven away from $NiAl_2O_4$ and formed NiO, which would be easily reduced to metallic Ni during the DRM reaction; whereas the direct formation of NiO and Al_2O_3 from the decomposition of $NiAl_2O_4$ (R3), without H_2, would not have been favorable. This meant that Ce_2O_3 generated from CeO_2 might have assisted the reduction of $NiAl_2O_4$ by forming a stable $CeAlO_3$.

$$\Delta G° = \sum(\Delta G_f°)_{product} - \sum(\Delta G_f°)_{reactant} \quad \text{(equ. 1)}$$

where the ΔG° stands for the reaction Gibbs free energy, $(\Delta G_f°)_{product}$ stands for the standard Gibbs free energy of the formation of product, and $(\Delta G_f°)_{reactant}$ stands for the standard Gibbs free energy of the formation of reactants.

$$Ce_2O_3 + Al_2O_3 \rightarrow 2CeAlO_3 \quad \text{(R1)}$$

$$Ce_2O_3 + NiAl_2O_4 \rightarrow 2CeAlO_3 + NiO \quad \text{(R2)}$$

$$NiAl_2O_4 \rightarrow Al_2O_3 + NiO \quad \text{(R3)}$$

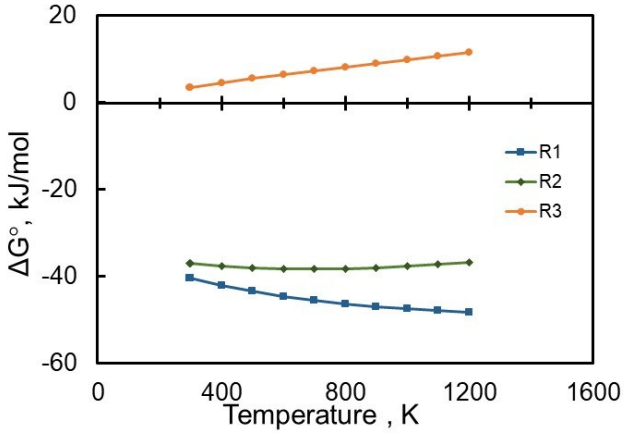

Figure S10. Gibbs free energy change as a function of temperature for solid phase reactions.

Verification of the possibility of $CeAlO_3$ formation

To verify the possibility of $CeAlO_3$ formation under DRM reaction conditions, XRD (as shown in Figure S11a) was conducted on $NiAl_2O_4$ (N1), CeO_2-$NiAl_2O_4$ (N2), and reduced CeO_2-$NiAl_2O_4$ (N3) as shown in Figure S11b. From Figure S11a, strong peaks for spinel $NiAl_2O_4$ were found. The peaks at 2θ=31.5°, 37.0°, 45.0°, 59.7°, and 65.6° corresponded to the (220), (311), (400), (511), and (440) planes of $NiAl_2O_4$. As CeO_2 was introduced to $NiAl_2O_4$ (CeO_2-$NiAl_2O_4$, N2), the peaks for CeO_2 appeared, including peaks at 2θ=28.5°, 47.6°, and 56.3° for the (111), (220), and (311) planes of CeO_2, respectively. When CeO_2-$NiAl_2O_4$ was reduced, strong peaks for the metallic Ni appeared, whereas the peak for $NiAl_2O_4$ became much weaker, indicating the reduction of $NiAl_2O_4$. In addition, peaks at 23.4°, 33.4°, 41.3°, 60.0°, and 70.4° were identified as the (001), (101), (111), (112), and (202) planes of $CeAlO_3$, whereas the peaks for CeO_2 became weaker and no peaks were observed for Ce_2O_3. This confirmed the reduction of CeO_2 and the possibility of formation of $CeAlO_3$ during the reaction condition.

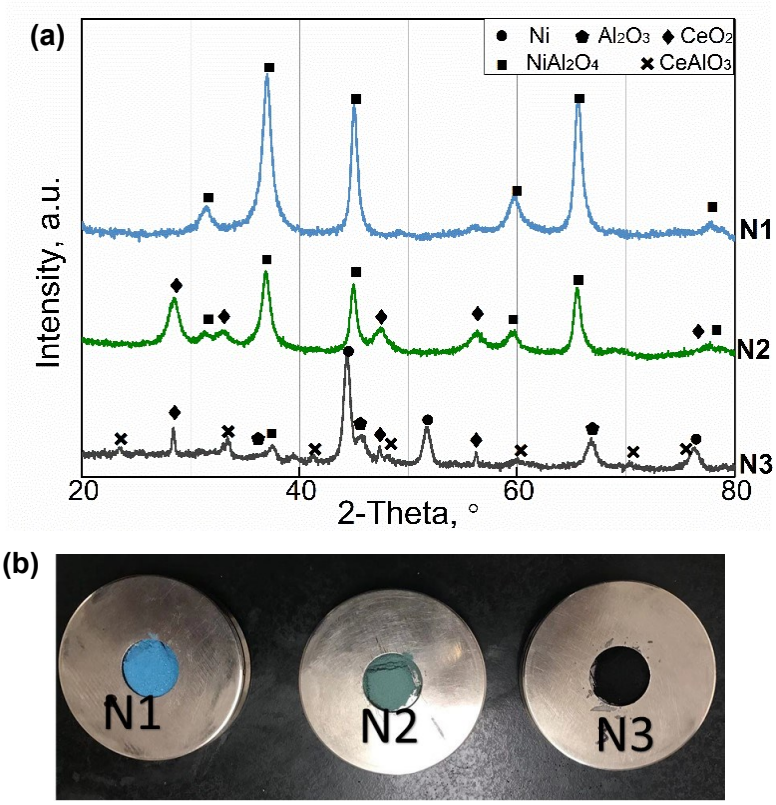

Figure S11. (a) XRD patterns and (b) pictures of $NiAl_2O_4$ (N1), CeO_2-$NiAl_2O_4$ (N2), and reduced CeO_2-$NiAl_2O_4$ (N3).

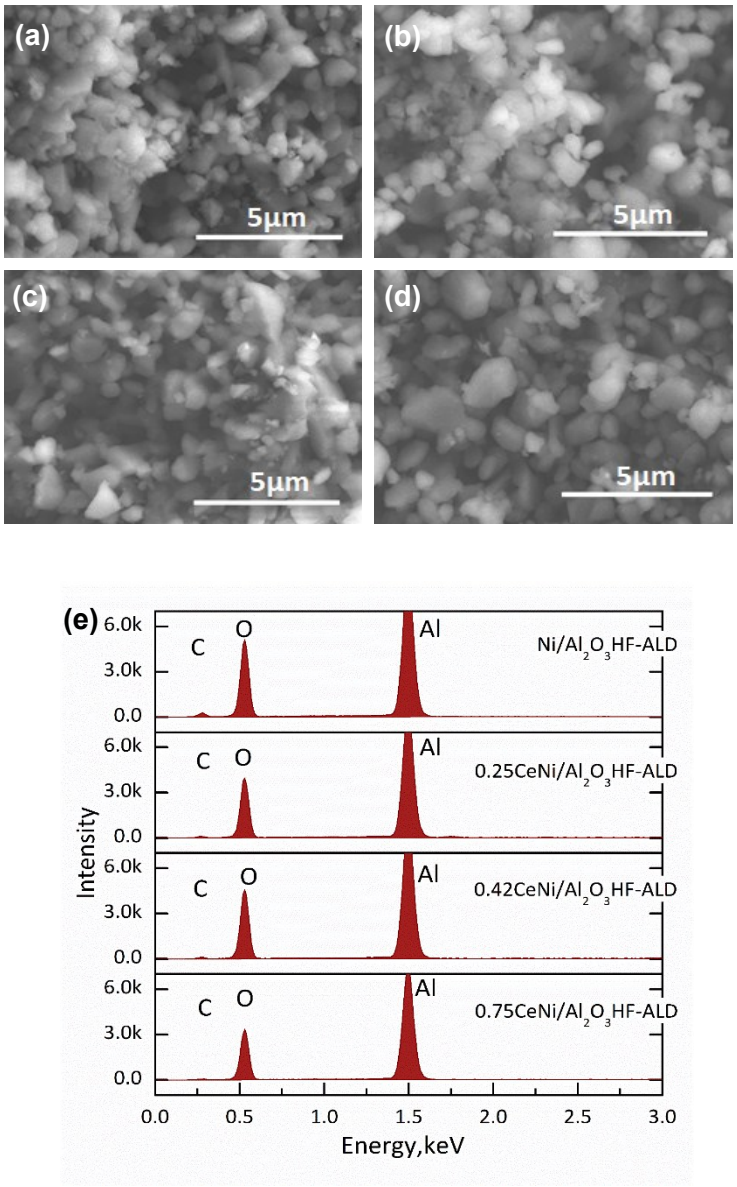

Figure S12. (a, b, c, d) SEM images of spent catalysts after two cycles of reaction and (e) EDS elemental analysis: (a) Ni/Al_2O_3HF-ALD, (b) 0.25CeNi/Al_2O_3HF-ALD, (c) 0.42CeNi/Al_2O_3HF-ALD, and (d) 0.75CeNi/Al_2O_3HF-ALD.

Table S1. Fitting results of XPS for $NiAl_2O_3$NP-ALD, $CeNiAl_2O_3$NP-ALD, spent $NiAl_2O_3$NP-ALD, and spent $CeNiAl_2O_3$NP-ALD, after DRM at 850 °C for 72 h.

Sample	Signal	Position, eV	FWHM, eV	Atomic, %	Assignment
$NiAl_2O_3$NP-ALD	C1s	284.5	1.6	71.6	C=C
		286.3	1.6	15.8	C-O
		288.5	1.6	12.6	C=O
	Ni 2p 3/2	853.2	2.2	4.9	Ni
		855.2	2.2	31.8	NiO
		856.4	2.2	17.5	$NiAl_2O_4$
		858.8		8.1	Ni(0) satellite
		861.2		37.6	Ni(II) satellite
	O 1s	530.5	1.6	65.8	Lattice oxygen
		531.4	1.6	23.2	Surface oxygen
		532.6	1.6	11.0	Adsorbed oxygen
$CeNiAl_2O_3$NP-ALD	C1s	284.5	1.6	75.5	C=C
		286.1	1.6	11.4	C-O
		288.4	1.6	12.1	C=O
	Ni 2p 3/2	854.3	2.3	35.8	NiO
		856.0	2.3	20.8	$NiAl_2O_4$
		860.8		43.4	Ni(II) satellite
	O 1s	530.1	1.6	59.1	Lattice oxygen
		530.9	1.6	32.5	Surface oxygen
		532.4	1.6	8.4	Adsorbed oxygen
	Ce 3d	881.4	2.6	22.7	v, 3d 5/2, Ce^{4+}
		884.6	2.6	7.7	v', 3d 5/2, Ce^{3+}
		887.6		13.1	v'', 3d 5/2, satellite
		897.4		16.5	v''', 3d 5/2, satellite
		900.0	2.6	15.2	u, 3d 3/2, Ce^{4+}
		902.8	2.6	5.1	u', 3d 3/2, Ce^{3+}
		906.3		8.7	u'', 3d 3/2, satellite
		915.8		11.0	u''', 3d 3/2, satellite
Spent $NiAl_2O_3$NP-ALD	C1s	284.5	1.4	83.6	C=C
		286.1	1.4	10.9	C-O
		288.3	1.4	5.5	C=O
	Ni 2p 3/2	852.6	2.0	39.4	Ni
		854.6	2.0	7.3	NiO
		856.1	2.0	20.5	$NiAl_2O_4$
		858.4		20.7	Ni(0) satellite
		861.5		12.2	Ni(II) satellite
	O 1s	530.6	1.6	77.8	Lattice oxygen
		531.4	1.6	14.1	Surface oxygen
		532.7	1.6	8.1	Adsorbed oxygen

Spent $CeNiAl_2O_3$NP-ALD	C1s	284.5	1.8	65.7	C=C
		286.1	1.8	21.5	C-O
		288.4	1.8	12.8	C=O
	Ni 2p 3/2	852.3	2.0	29.2	Ni
		854.3	2.0	18.7	NiO
		856.1	2.0	12.4	$NiAl_2O_4$
		858.3		27.8	Ni(0) satellite
		861.3		12.0	Ni(II) satellite
	O 1s	530.4	1.7	48.7	Lattice oxygen
		531.5	1.7	39.5	Surface oxygen
		532.6	1.7	11.8	Adsorbed oxygen
	Ce 3d	881.4	2.6	20.8	v, 3d 5/2, Ce^{4+}
		884.8	2.6	27.4	v', 3d 5/2, Ce^{3+}
		886.7		4.6	v'', 3d 5/2, satellite
		897.9		7.2	v''', 3d 5/2, satellite
		900.2	2.6	13.9	u, 3d 3/2, Ce^{4+}
		903.3	2.6	18.3	u', 3d 3/2, Ce^{3+}
		906.2		3.0	u'', 3d 3/2, satellite
		916.1		4.8	u''', 3d 3/2, satellite

References:

1. A. Remiro, A. Arandia, L. Oar-Arteta, J. Bilbao and A. G. Gayubo, *Appl. Catal. B: Environ*, 2018, **237**, 353-365.
2. B. Ihsan, *Thermochemical Data of Pure Substances, third ed.*, Weinheim, New York, 1995.